LAWRENCE
LIVERMORE
NATIONAL
LABORATORY

Synchrotron Based Observations of Sigma Phase Formation and Dissolution in Duplex Stainless Steel

J. Elmer, T. Palmer, E. Specht

August 23, 2006

Disclaimer

This document was prepared as an account of work sponsored by an agency of the United States Government. Neither the United States Government nor the University of California nor any of their employees, makes any warranty, express or implied, or assumes any legal liability or responsibility for the accuracy, completeness, or usefulness of any information, apparatus, product, or process disclosed, or represents that its use would not infringe privately owned rights. Reference herein to any specific commercial product, process, or service by trade name, trademark, manufacturer, or otherwise, does not necessarily constitute or imply its endorsement, recommendation, or favoring by the United States Government or the University of California. The views and opinions of authors expressed herein do not necessarily state or reflect those of the United States Government or the University of California, and shall not be used for advertising or product endorsement purposes.

SYNCHROTRON BASED OBSERVATIONS OF SIGMA PHASE FORMATION AND DISSOLUTION IN DUPLEX STAINLESS STEEL

J. W. Elmer, T. A. Palmer and E. D. Specht*

Lawrence Livermore National Laboratory, Livermore, CA
*Oak Ridge National Laboratory, Oak Ridge, TN

ABSTRACT

The formation and growth of sigma (σ) phase in 2205 duplex stainless steel was observed and measured in real time using synchrotron radiation during isothermal heat treating at temperatures between 700ºC and 850ºC. Synchrotron experiments were performed on this material at the Advanced Photon Source (APS) while isothermally holding the samples for times of up to 10 hr. During the isothermal hold, sigma formed in quantities up to 22% as the ferrite transformed to a mixture of sigma and austenite phases. In addition, sigma formed at 850ºC was heated to 1000ºC to observe its dissolution. The amounts of sigma that formed, and the dissolution temperature of sigma were compared to the results predicted by Thermocalc, showing differences between the calculated and measured values. The synchrotron data was further modeled using a modified Johnson-Mehl-Avrami analysis to determine kinetic parameters for sigma formation. The initial JMA exponent, n, at low fractions of sigma was found to be approximately 7.0, however, towards the end of the transformation, n decreased to values of approximately 0.75. Because of the variable value of n, it was not possible to determine reliable values for the activation energy and pre-exponential terms for the JMA equation. During cooling to room temperature, the high temperature austenite partially transformed to ferrite, substantially increasing the ferrite content while the sigma phase kept its high temperature value.

INTRODUCTION

Duplex stainless steels (DSS) are often processed to have nearly equal amounts of ferrite and austenite in the microstructure, which provides them with a desirable combination of strength, toughness, and corrosion resistance [1]. However, when exposed to elevated temperatures between approximately 600ºC and 1000ºC for sustained periods of time, several undesirable intermetallic phases can form [2, 3]. The σ phase, which has a complex tetragonal crystal structure with a large unit cell, is the most prominent of the intermetallic phases. Sigma is enriched in Cr and Mo relative to the nominal composition

1

of the alloy, and because of this it grows from the ferrite phase which is also enriched in these elements [1, 4].

Once formed, sigma is known to adversely affect the mechanical properties [4-8] and corrosion resistance [9, 10] of DSS alloys. For example, the impact toughness of 2205 DSS has been found to decrease by nearly an order of magnitude when exposed to an extended 850ºC isothermal heat treatment [6]. Decreases in the pitting and crevice corrosion resistance are also pronounced in the presence of σ phase. This decrease in corrosion resistance is attributed to the regions surrounding the newly formed sigma precipitates which are depleted of Mo and Cr [10]. As a result, the DSS becomes susceptible to localized corrosion via a mechanism similar to sensitization observed in austenitic stainless steels.

During elevated temperature processing of DSS, sigma preferentially nucleates heterogeneously at either austenite/ferrite or at ferrite/ferrite grain boundaries that are present in the starting microstructure. The amount of ferrite that forms depends on both the alloy composition and the amount of ferrite in the starting microstructure. Sigma phase has been observed in cast alloys [11, 12], in weld metal fusion and heat affected zones [13-15], and in continuously cooled [16] duplex stainless steels, indicating its propensity to form under numerous materials processing conditions.

In this investigation, high intensity synchrotron x-ray radiation is used to directly observe the transformation of ferrite to sigma phase and secondary austenite in 2205 DSS, and to observe the dissolution of sigma at temperatures approaching 1000ºC. The results from these experiments are used to determine the kinetics of σ formation and dissolution, and help to provide a sound basis for the design of DSS alloys for a given application without significant degradation of properties.

EXPERIMENTAL PROCEDURES

MATERIALS

Chemical analysis performed on the 2205 DSS used in this study shows that it contains 22.43%Cr, 4.88%Ni, 3.13%Mo, 0.14% Mn, 0.67%Si, 0.18%N and 0.023%C by weight. This is the same material used during previous investigations where synchrotron radiation was employed to observe phase transformations during welding [17, 18]. The as-received material had been solution mill annealed at 1065ºC for 2.5 hrs followed by water quenching to produce a balanced ferrite/austenite microstructure. All of the samples were removed from the 10.8 cm diameter bar along the direction of extrusion. The sample geometry was the same as that used in other experiments, measuring 100 mm long by 4.75 mm wide and 2 mm thick [19, 20].

Fig. 1 shows the heat treated microstructure after an 850ºC isothermal hold for 10 hrs. This microstructure was revealed using an electrolytic KOH etch (50 gm KOH, 100 mL water) held at a voltage of 5V for approximately 10 s [11]. Here sigma is present in volume

fractions near 20%, and is the most darkly etched phase (brown/orange/black) in the microstructure. The ferrite etches a blue/purple color and the austenite etches a tan/grey color.

THERMODYNAMICS

ThermoCalc® version q and the TC Fe2 database was used to calculate the phase equilibria in the 2205 DSS alloy. The model considered the effects of Fe, Cr, Ni, Mo, Mn, Si, C, and N, on the presence of ferrite, austenite, sigma, nitrides/carbides, and the liquid phases. Fig. 2 shows the resulting phase fraction versus temperature plot, indicating that ferrite transforms to a combination of austenite and sigma during heating up to 700ºC. Between 700ºC to 800ºC the ferrite does not exist, yet the sigma partially transforms to austenite as the temperature increases. At 800ºC ferrite begins to form again, and sigma continues to decrease until it completely disappears at a temperature of approximately 860ºC. At higher temperatures, ferrite increases and austenite decreases until they have equal amounts at 1065ºC. Since the microstructure of the initial 2205 DSS is metastable due to its quenching from elevated temperatures, the real microstructure starts off with a significantly different ferrite/austenite ratio than that predicted from the thermodynamic calculations.

IN-SITU X-RAY DIFFRACTION EXPERIMENTS

Two types of *in-situ* x-ray diffraction experiments were performed while heating test coupons in vacuum using a direct resistance method [19-21]. In the first series, samples were heated to predetermined temperatures between 700ºC and 850ºC and held at this temperature for periods up to 10 hr to observe the isothermal transformation of ferrite to sigma and austenite. In the second, the sample was heated to the initial temperature of 850ºC where it was held for 30 min to form a measurable amount of sigma. The sample was then ramped to 1000ºC and back to 850ºC at a slow rate of 0.25ºC/s to determine the temperature where sigma dissolves. After ramping to and from 1000ºC, the sample was held at 850ºC for an additional 30 minutes to observe the re-formation of sigma before cooling the sample back to room temperature at approximately 20 ºC/s.

The experiments were performed at the Advanced Photon Source (APS) at the Argonne National Laboratory on the UNICAT beam line BM-33-C. This beam line produced a 30keV x-ray beam that was adjusted to a size of 1.0 mm wide by 0.25 mm high using vertical and horizontal slits. A schematic diagram of the experimental setup is shown in Fig. 3, showing the environmental chamber that is pumped down to 10 mtorr prior to starting the experiment, the water cooled grip sample holder, Type S thermocouple and the sample inside. During the experiment, the x-ray beam passes through a kapton window and impinges on the top surface of the sample at a 5° angle of incidence. Diffraction takes place on the surface of the sample and the diffracted beams pass through a second kapton window behind the sample before being collected by a CCD detector placed 330 mm behind the sample. The detector was manufactured by Roper Scientific (A99k401, RS/Photometrics) and uses a 6.1 x 6.1 cm^2 array of 1024x1024 pixels spaced 60 microns apart, and was set to integrate the diffraction patterns over a 1 s exposure time. The detector requires an

additional 2 s to clear the data from the CCD detector and transfer it to the computer. After the data was recorded, the Debye arcs were converted into a conventional diffraction plot to show the diffracted beam intensity versus d-spacing using Fit-2D software. Additional details about the data acquisition technique on this beam line are presented elsewhere [19, 20].

Figure 4 shows a room temperature diffraction pattern (upper line) taken after an 850ºC heat treatment where a significant amount of sigma phase has formed. Superimposed on this figure is a calculated diffraction pattern of the sigma phase (lower line) [21]. The results show that three austenite peaks, three ferrite peaks, and a multitude of sigma peaks should appear in the diffraction window. All of the non-fcc or non-bcc peaks can be attributed to the sigma phase, and it can be seen that the sigma (330), peak 3, overlaps with the fcc (111), and that the sigma (202), peak 4, overlaps with the bcc (110) peaks. A complete indexing of all of the diffraction peaks for this DSS alloy is presented elsewhere [21].

Once all the x-ray diffraction data was acquired, the peak areas were measured for each phase and used as a means to determine their relative amounts. The peaks used in this measurement were the three major bcc peaks, (110), (200), 220), and the three major fcc peaks, (111), (200), (220). In addition, six of the highest d-spacing peaks of the sigma phase were analyzed corresponding to the (002), (410), (212), (411), (331), and (222) reflections. The diffraction peaks were then converted into fractions of each phase by taking into account the structure factors for ferrite, austenite, and sigma phases, the multiplicity for each peak, and the Lorentz polarization factors as described elsewhere [21]. These calculations were performed on every diffraction pattern throughout the isothermal hold, allowing the volume fraction of each phase to be determined as a function of isothermal hold time.

RESULTS

SIGMA FORMATION DURING ISOTHERMAL HEATING

The isothermal experiments were performed according to the time-temperature profiles listed in Table 1. In this table, the different temperatures, holding times and amounts of each phase at the beginning and end of the isothermal hold are given. In addition, the volume fraction of each phase is listed at the beginning and end of each heat treatment, and the time at which sigma phase was first observed is also shown. These results are summarized from the *in-situ* x-ray diffraction patterns such as the one shown in Fig. 5, where the diffraction patterns are lined up with time along the y-axis, d-spacing along the X-axis, and the intensities of the diffraction peaks represented by different colors. In this figure, the initial 2000 s of the run at 800ºC is plotted, from t=0 s where heating initiates through the formation of a significant amount of sigma phase. As soon as the sample begins to heat, the fcc and bcc diffraction peaks shift to higher d-spacings due to the thermal expansion effect. During the isothermal hold, which begins at t=48 s, the intensity of the bcc peak immediately begin to decrease while the intensity of the fcc peaks increase. At t=96 s, the

sigma (410) peak first appears, but at low intensity. With increased holding time this peak intensifies and additional sigma peaks appear as the sigma phase grows.

The changes in the diffraction peak intensity can be correlated with changes that are taking place in the volume fractions of each of the three phases during the isothermal hold [21]. Fig. 6 plots the measured volume fractions of these phases as a function of isothermal heat treatment time for the first hour of the hold where the majority of the transformation takes place at 800ºC. The alloy begins with a ferrite/austenite ratio of approximately 1:1, which decreases considerably as ferrite partially transforms to austenite and sigma phases. Sigma, which first appears at t=96 s, rapidly increases to approximately 90% of its equilibrium value within the first 1 hr of the run. Similar transformations were observed at the other isothermal hold temperatures. However, the rates of transformation and amounts of sigma phase produced varied with temperature.

Figure 7 compares the measured amounts of sigma phase as a function of time for each of the four isothermal holds. The amount of sigma formed varies from 19.8% to 22.7%, as summarized in Table 1, with the lowest amount of sigma being found at the highest temperature (850ºC). Equilibrium volume fractions appear to be reached at all of the temperatures except 700ºC. The data was further plotted in Fig. 8 to show the time temperature relationships for the formation of sigma phase at seven different amounts of transformation, between 1% to 99%. In this plot, the measured maximum amount of sigma that formed at each temperature was used to represent 100% of the possible amount of sigma that could form (see Table 1), and this value decreased with increasing temperature. This plot clearly indicates C-curve kinetics with the nose of the transformation occurring at approximately 800ºC.

Table 1 compared the measured amounts of sigma phase with those predicted by Thermocalc, and showed significant differences between the two. The measured amounts of sigma phase for the three temperatures where near equilibrium amounts of sigma formed (750ºC, 800ºC and 850ºC) exceed those predicted by Thermocalc. At 750 and 800ºC, the difference is only a few percent. At 850ºC, however, the difference is nearly a factor of 6. Since the amount of sigma phase decreases to zero at temperatures above its solvus, a reduction in the amount of sigma is expected at higher temperatures. However, the temperature at which the rapid decrease in sigma occurs appears to be underpredicted by Thermocalc. Whereas Thermocalc predicts zero percent sigma at 860ºC, the synchrotron measurements show approximately 15% sigma at this temperature. Taking this data all together, it appears as though Thermocalc is underpredicting the sigma dissolution temperature by approximately 50ºC.

ISOTHERMAL KINETICS OF SIGMA PHASE FORMATION

Analysis of the synchrotron data on the 2205 DSS was performed using a Johnson Mehl Avrami (JMA) method to describe the overall transformation rate. This approach can be represented by the following expression [22]:

$$f_e(t) = 1 - \exp\{-(kt)^n\} \qquad \text{(eq. 1)}$$

where $f_e(t)$ is the extent of the transformation as a function of time t measured relative to the equilibrium value of the product phase, n is the JMA exponent, and k is a rate constant given as:

$$k = k_0 \exp(-\frac{Q}{RT}) \qquad \text{(eq. 2)}$$

In this expression, k_0 is a pre-exponential constant, Q is the activation energy of the transformation including the driving forces for both nucleation and growth, R is the gas constant and T is the absolute temperature (K). The JMA exponent, n, is often correlated to different types of nucleation and growth conditions, and is an indicator of the kinetics responsible for the transformation [23].   One way to determine the value of the JMA exponent from experimental data is to linearize eq. (1) by plotting the $\ln(\ln(1-f_e(t)))$ versus ln(t), where n can be determined from the slope of the data.

Figure 9 plots the fraction sigma phase formed for each of the four temperatures on the JMA coordinates. In this plot it is clear that the data do not follow a linear trend with ln(t), and that all of the curves start off with a steep slope that decreases as the transformation continues. The initial slope, between 1% and 5% sigma, for each of the four sets of data is summarized in Table 2. These slopes give the JMA exponent, n, to be approximately 7.0.   However, n continuously decreases and towards the end of the transformation, n approaches a value of approximately 0.75 at the three highest temperatures where the transformation went to completion. This change in slope indicates a change in the JMA exponent, and suggests that the mechanism for the transformation is changing as the transformation proceeds. Because of this, reliable values of the activation energy, Q, and the JMA pre-exponential term, ko, were not able to be determined for this transformation. However, the changing slope and its value are useful information nevertheless since this information can be used as an indicator of the type of nucleation and growth conditions that are occurring.

According to Christian [23], a JMA exponent above 4, like those observed at low fractions of sigma, would indicate that the transformation is taking place by either a discontinuous precipitation or an interface controlled growth mechanism, with a nucleation rate that increases with increasing fraction transformed. At longer transformation times, the JMA exponent decreases to values of approximately 0.75, which can indicate thickening of large plates or growth of particles after nucleation site saturation was achieved [23]. This transformation mechanism would occur when the majority of available nucleation sites are already taken and the transformation continues by growth of the existing sigma phase particles. Thus, the formation of sigma phase in this alloy is one that appears to be strongly influenced by the nucleation conditions since growth of the sigma phase is slow at these temperatures. Even at the highest temperatures and longest isothermal hold times (see Fig 1), the sigma phase particles retain their individual shapes, and never appear to grow larger than about 10 μm in size.

AUSTENITE TO FERRITE TRANSFORMATION DURING COOLING

During the isothermal hold, the ferrite transformed to a mixture of austenite and ferrite phases, and the maximum amount of ferrite at the end of the hold varied with temperature. The highest amount of ferrite at the end of the hold was only 3.2% for the sample held at 700ºC, and the lowest amount of ferrite was near 0% in the sample held at 800ºC. However, after the samples had been cooled back to room temperature, the microstructure revealed a significant amount of ferrite present in each. Fig 1 showed the post heat treated microstructure of the sample held at 850ºC, clearly indicating the presence of large amounts of ferrite, on the order of 30%. The ferrite that appears in the sample after heat treating was created by the back transformation of austenite to ferrite during cooling to room temperature. This partial transformation of austenite to ferrite is expected based on the thermodynamic calculations shown in Fig 2, which indicate that austenite begins to transform to ferrite at temperatures below about 700ºC.

The amount of ferrite that re-formed in one of the samples (800ºC) was monitored during cooling to follow the phase transformations back to room temperature. Figure 10 shows the results of this measurement and compares the ferrite, austenite and sigma phase contents from the start to the end of the run. This plot shows that the austenite in the starting material (49.6%) increased to 79.8% during the isothermal hold, but then decreased to 45.1% during cooling to room temperature. Thus the final amount of austenite in this sample is only slightly less than the initial amount. The ferrite on the other hand has an initial value of 50.4% which rapidly decreased to near-zero values during the isothermal hold. During cooling, the ferrite increased to 34.7% as the amount of austenite decreased. While the austenite was transforming to ferrite during cooling, the sigma phase did not transform at all, retaining 20.2% sigma phase at room temperature. In the end there was a net decrease in the ferrite content of the sample of 15.7% and a net decrease in the austenite of 4.5%, which was compensated for by the retained sigma phase at room temperature of 20.2% in this sample. Thus, the direct observation of the phases existing at elevated temperature made possible with *in-situ* x-ray diffraction provides confirming evidence of the phases and condition that are not present in post experimental observations.

SIGMA PHASE DISSOLUTION AND RE-FORMATION

One of the samples was used to observe the formation and dissolution of sigma phase. This sample was heated at a rate of 20ºC/sec to an initial temperature of 850ºC where it was held for 30 min to form a measurable amount of sigma. The sample was then ramped to 1000ºC and back to 850ºC at a slow rate of 0.25ºC/s to determine the temperature where sigma dissolved. After ramping to and from 1000ºC, the sample was held at 850ºC for an additional 30 min to observe the re-formation of sigma before cooling the sample back to room temperature at approximately 20ºC/s. Figure 11 shows the results of the x-ray diffraction data plotted for the initial 3700 s of the run, over the d-spacing range where the most important sigma phase peaks appear. In this plot, the series of diffraction patterns are plotted with time along the y-axis, d-spacing along the x-axis, and the intensities of the

diffraction peaks represented by different colors. The heating initiates at t=0 s, and immediately all of the fcc and bcc diffraction peaks shift to higher d-spacings due to the thermal expansion effect while the sample is being heated to 850ºC. During holding, the intensity of the bcc peaks immediately began to decrease while the intensity of the fcc peaks increased. At t=81s, the first sigma peak (411) appears, 40s into the isothermal hold. With increased holding time this peak intensifies and additional sigma peaks develop, reaching a maximum of 13.4%. The ramp to 1000ºC begins at t=1850 s, reaching 1000ºC at t=2450 s. As the temperature ramps up the amount of sigma decreases, eventually reaching 0% at a temperature of 985ºC. Sigma does not reappear again until the sample has been cooled back down and held at 850ºC.

A summary of the measured fractions of sigma, ferrite and austenite is shown in Fig. 12, including the temperature profile for this experiment. It is clear that sigma forms in increasing amounts until the temperature begins to ramp from 850ºC to 1000ºC, reaching 0% at 985ºC. This observed dissolution temperature for sigma is more than 100ºC higher than predicted by thermodynamics. The difference is most likely a combination of some inaccuracies in the thermodynamics, the fact that the sample was being heated a constant rate so that the observed dissolution temperature is somewhat above its true equilibrium value, and possible errors in the temperature measuring accuracy.

The accuracy of the temperature measurement is only a few degrees centigrade, and can be estimated from the accuracy of the Type S thermocouple plus any uncertainty in the timing between the temperature measurement and the integration time of the x-ray detector. The thermocouple accuracy is stated to be 0.25% of the measured value or 1.5ºC, whichever is greater, and this factor becomes 2.5ºC at 1000ºC. The uncertainty based on the x-ray detector timing is the heating rate (0.25ºC/s) multiplied by the x-ray integration time (1 s), which is 0.25ºC. Adding these two values together gives a total measurement uncertainty of the dissolution temperature of 2.75ºC, so this in not believed to be a major contribution to the observed dissolution temperature difference.

Although the heating rate of this sample is fairly slow at 0.25ºC/s, it would still be expected that there is some overshoot of the temperature due to kinetic effects before sigma dissolves completely. With only one heating rate examined here, it is not possible to determine how much superheat can be attributed to the heating rate effect, and additional experiments are planned at different heating rates to study this effect.

The third contribution to the difference in the measured and calculated dissolution temperature is the accuracy of the thermodynamic calculations themselves. Although this is not a known factor, there is evidence in the measured data that the thermodynamic calculations are underpredicting the dissolution temperature. Although the thermodynamics predicts the equilibrium fraction of sigma to be only 3.4%, 13.4% sigma is measured after 30 min of holding at 850ºC, and nearly 20% is expected to form at longer holding times [13]. This difference can only be explained if the thermodynamics are underpredicting the sigma dissolution temperature. Another indication is that the ferrite calculations also appear to be off. Thermodynamics predicts ferrite to be in excess of 20% at 850ºC, but the measured value was only 13% and was decreasing with additional holding time.

After reaching 850ºC it took 186 s before the first sigma was observed. This time is more than 4 times longer than that required during the initial heating stage (40 s). In

addition to the longer time required for sigma to appear, the rate of sigma formation was significantly reduced after cooling down from 1000ºC. As indicated in Fig. 7, 13.4% sigma was formed during the first 1800s hold, whereas only 5.4% sigma formed during the same amount of time after cooling down from 1000ºC. The slower kinetics are most likely related to homogenization that takes place at the higher temperature which reduces the concentration of Cr and Mo. In addition there is a possible decrease in the number of preferred nucleation sites for sigma since some grain growth would have taken place at 1000ºC to reduce the amount of grain and phase boundaries.

CONCLUSIONS

1. The formation and growth of sigma phase in 2205 DSS was observed and measured in real time using synchrotron radiation during isothermal heat treating at temperatures between 700ºC and 850ºC, and for times up to 10 hr.
2. Ferrite was observed to transform to a mixture of sigma and austenite during the 10 hr hold times. The measured amounts of sigma were compared to those predicted by Thermocalc version q using the TCFe2 database. Differences between the calculated and measured amounts of sigma suggest that the thermodynamic calculations underpredict the maximum temperature where sigma can exist by about 50ºC
3. A TTT diagram was created for the sigma phase transformation, showing that the nose of the curve is at approximately 800ºC, which is similar to the results from other investigators who find the nose at temperatures between 800ºC and 850ºC.
4. A JMA analysis of the sigma phase transformation kinetics revealed that the transformation rates were significantly different at low and high amounts of sigma phase. At low sigma fractions, the initial JMA exponent, n, was found to be approximately 7.0. However, n was shown to continuously decrease to values of approximately 0.75 near the end of the transformation. Reliable values of the activation energy, Q, and the JMA pre-exponential term, ko, were not able to be determined for the transformation due to this variation in n.
5. The change in the JMA exponent with the amount of sigma formed was attributed to changes in the transformation mechanism whereby the higher values during the early stages of transformation corresponded to discontinuous precipitation mechanism with increasing nucleation rate, the lower values during the later stages of the transformation corresponded to growth of the existing sigma phase after nucleation site saturation occurred.
6. The back transformation of austenite to ferrite during cooling after the isothermal hold was measured, showing that the austenite decreases back to near its original value after the sample has cooled and the ferrite increases to an amount significantly less than its original value, while sigma maintained its high temperature value when cooled to room temperature.
7. Dissolution of sigma at 850ºC was observed to occur at 985 ±2.8ºC while heating at the rate of 0.25ºC/s. This temperature is more than 100ºC higher than the value predicted by thermodynamic calculations.

8. The kinetics of sigma formation at 850ºC were significantly slower after dissolution at 1000ºC than before. This change is likely related to homogenization that took place at the peak temperature plus a reduction in the amount of preferred sigma nucleation sites.

REFERENCES

1. H.D. Solomon and T.M. Devine, "Duplex Stainless Steels – A Tale of Two Phases," in *Duplex Stainless Steels*, ed. by R.D. Lula, American Society for Metals, Metals Park, OH, 1983, pp. 693-756.
2. L. Karlsson, "Intermetallic Phase Precipitation in Duplex Stainless Steels and Weld Metals: Metallurgy, Influence on Properties, Welding and Testing Aspects"*, WRC Bulletin,* 438 (1999).
3. J.-O. Nilsson, "Super Duplex Stainless Steels", *Mater. Sci. Technol.*, 8, (1992), 685-700.
4. E. O. Hall and S. H. Algie, "The Sigma Phase," *Metallurgical Reviews*, Review No. 104, The Institute of Metals, Vol (11), (1966), 61-88.
5. J.-O. Nilsson, P. Kangas, T. Karlsson, and A. Wilson, "Mechanical Properties, Microstructural Stability and Kinetics of σ -Phase Formation in 29Cr-6Ni-2Mo-0.38N Superduplex Stainless Steel", *Metall.Mater. Trans A*, 31A, (2000), 35-45.
6. Y.S. Ahn and J.P. Kang, "Effect of Aging Treatments on Microstructure and Impact Properties of Tungsten Substituted 2205 Duplex Stainless Steel", *Mater. Sci. Technol.*, 16, (2000), 382-388.
7. J. Li, T. Wu, and Y. Riquier, "σ Phase Precipitation and its Effect on the Mechanical Properties of a Super Duplex Stainless Steel", *Mater. Sci. Engin.*, A174, (1994), 149-156.

8.   T.H. Chen, K.L. Weng, and J.R. Yang, "The Effect of High-Temperature Exposure on the Microstructural Stability and Toughness Property in a 2205 Duplex Stainless Steel", *Mater. Sci. Engin. A*, A338, (2002), 259-270.

9.   J.-O. Nilsson and A. Wilson, "Influence of Isothermal Phase Transformations on Toughness and Pitting Corrosion of Super Duplex Stainless Steel SAF 2507", *Mater. Sci. Technol.*, 9, (1993), 545-554.

10. Y.S. Ahn, M. Kim, and B.H. Jeong, "Effect of Aging Treatments and Microstructural Evolution on Corrosion Resistance of Tungsten Substituted 2205 Duplex Stainless Steel", *Mater. Sci. Technol.*, 18, (2002), 383-388.

11. E. Johnson, Y-J. Kim, L.S. Chumbley, and B. Gleeson, "Initial Phase Transformation Diagram Determination for the CD3MN Cast Duplex Stainless Steel", *Scripta Mater*, 50, (2004), 1351-1354.

12. Y-J. Kim, L.S. Chumbley, and B. Gleeson, "Determination of Isothermal Transformation Diagrams for Sigma-Phase Formation in Cast Duplex Stainless Steels CD3MN and CD3MWCuN", *Metall. Mater. Trans. A*, 35A, (2004), 3377-3386.

13. J.-O. Nilsson, T. Huhtala, P. Jonsson, L. Karlsson, and A. Wilson, "Structural Stability of Super Duplex Stainless Steel Weld Metals and Its Dependence on Tungsten and Copper", *Metall. Mater. Trans. A*, 27A, (1996), 2196-2208.

14. J.M. Vitek and S.A. David, "The Aging Behavior of Homogenized Type 308 and 308CRE Stainless Steel", *Metall. Trans. A*, 18A, (1987), 1195-1201.

15. T. H. Chen and J. R. Yang, "Microstructural Characterization of Simulated Heat Affected Zone in a Nitrogen-Containing 2205 Duplex Stainless Steel," Mat. Sci. Eng. A, (338), (2002), 166-181.

16. T. H. Chen and J. R. Yang, "Effects of Solution Treatment and Continuous Cooling of σ-Phase Precipitation in a 2205 Duplex Stainless Steel," *Materials Science and Engineering A*, (311), (2001), 28-41.

17. T. A. Palmer, J. W. Elmer, S. S. Babu, "Observations of Ferrite/Austenite Transformations in the Heat Affected Zone of 2205 Duplex Stainless Steel Spot Welds Using Time Resolved X-Ray Diffraction." *Materials Science and Engineering A*, Vol. 374, pp. 307-321, 2004.

18. T. A. Palmer, J. W. Elmer, and Joe Wong, "In-Situ Observations of Ferrite/Austenite Transformations in Duplex Stainless Steel Weldments Using Synchrotron Radiation," *Science and Technology of Welding and Joining*, Vol. 7(3), pp 159-171, 2002.

19. J.W. Elmer, T.A. Palmer, S.S. Babu, and E.D. Specht, "In-Situ Observations of Lattice Expansion and Transformation Rates of α and β Phases in Ti-6Al-4V", *Materials Science and Engineering A*, 391(1-2), 104-13 (2004).

20. J.W. Elmer, T.A. Palmer, S.S. Babu, and E.D. Specht, "Low Temperature Relaxation of Residual Stress in Ti-6Al-4V," *Scripta Materiallia*, 52 (10), 1051-6 (2005).

21. J. W. Elmer, T. A. Palmer and E. D. Specht, "Direct Observations of Sigma Phase Formation in Duplex Stainless Steels using In-Situ X-Ray Diffraction," Submitted to *Metallurgical and Materials Transactions A*, July, 2006.

22. J. W. Elmer, T. A. Palmer, W. Zhang, and T. DebRoy, "Advanced Techniques for In-Situ Monitoring of Phase Transformations During Welding Using Synchrotron-Based X-Ray Diffraction," 7*th International Conference on Trends in Welding Research, ASM International,* Pine Mountain Georgia, May, 2005.
23. J. W. Christian: *The Theory of Transformations in Metals and Alloys, 2nd Edition, Part I,* 1975, Oxford: Pergamon.

Table 1. Summary of volume fractions measured at the beginning of the heating cycle and at the end of the isothermal holds. The equilibrium values, as determined by Thermocalc, are shown for comparison.

Amount of Phase	Isothermal hold temperature			
	700ºC	750ºC	800ºC	850ºC
Start of hold				
Ferrite (%)	57.2	55.0	50.4	53.5
Austenite (%)	42.8	45.0	49.6	46.5
Time, first sigma (s)	2003	192	96	157
End of hold				
Time (s)	36070	25007	35951	36241
Ferrite (%)	3.2	0.29	.05	1.9
Austenite (%)	78.3	77.2	79.8	78.3
Sigma (%)	18.5*	22.7	20.2	19.8
Thermocalc				
Ferrite (%)	0	0	0	31.6
Austenite (%)	78.6	80.6	82.5	65.0
Sigma (%)	21.4	19.4	17.5	3.4

* Transformation not completed at end of 10 hour isothermal hold.

Table 2. Results of the JMA calculations of sigma formation at the four temperatures. Due to the changing value of n, the other JMA parameters could not be reliably determined.

Temperature (ºC)	n initial	n final
700	4.7	-
750	7.8	0.75
800	6.7	0.68
850	7.0	0.73
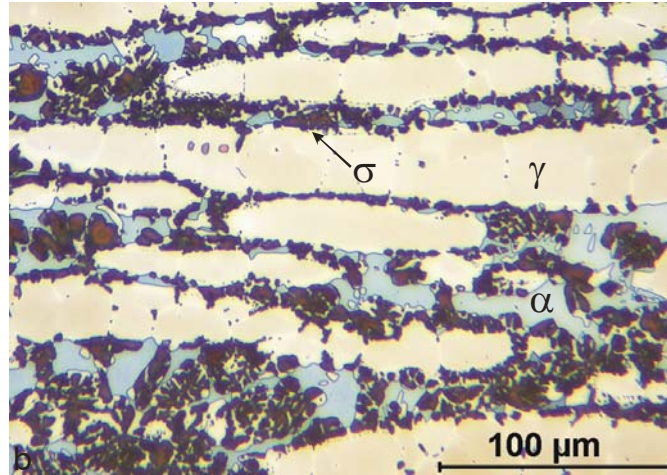
Figure 1: Optical micrographs showing the microstructure of the sample after the heat treating cycle. Ferrite, α, etches blue/purple in color, austenite, γ, etches tan/white in color, and σ phase etches black/brown in color.
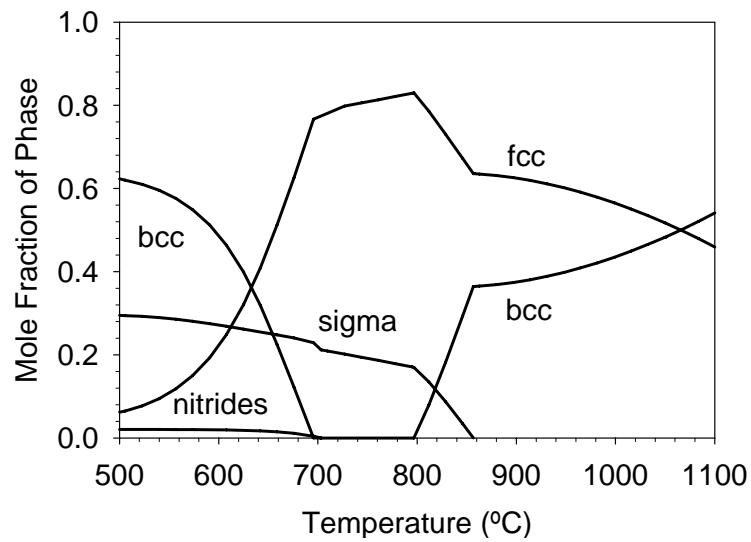

Figure 2: Calculated phase fractions for the 2205 DSS alloy used in this study. The sigma phase is predicted to be present only at temperatures below 860ºC. The Y-axis in plotted in mole fraction, where one mole is an Avogadro's number of total atoms.
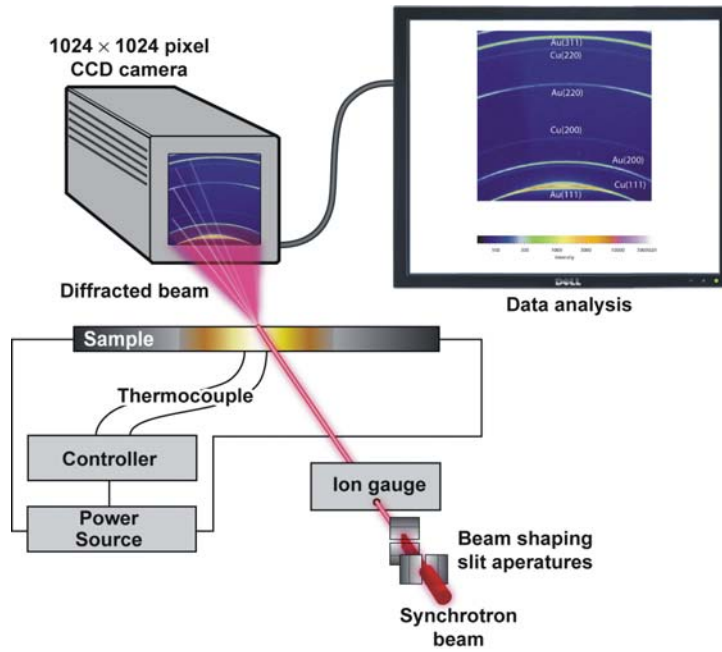
Figure 3:   Schematic diagram of the x-ray setup used for *in-situ* observations of phase transformations under controlled heating and cooling conditions.
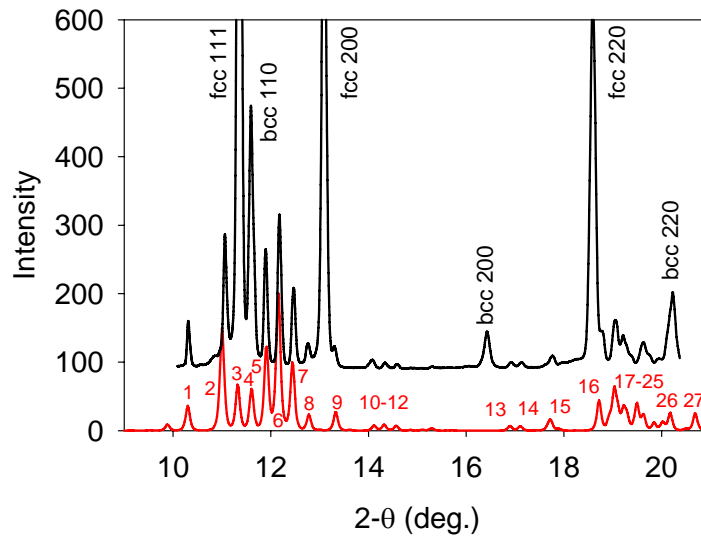
Figure 4:   Comparison of the measured room temperature diffraction pattern after heat treating showing bcc, fcc and sigma (upper pattern) with the calculated diffraction pattern of sigma (lower pattern).
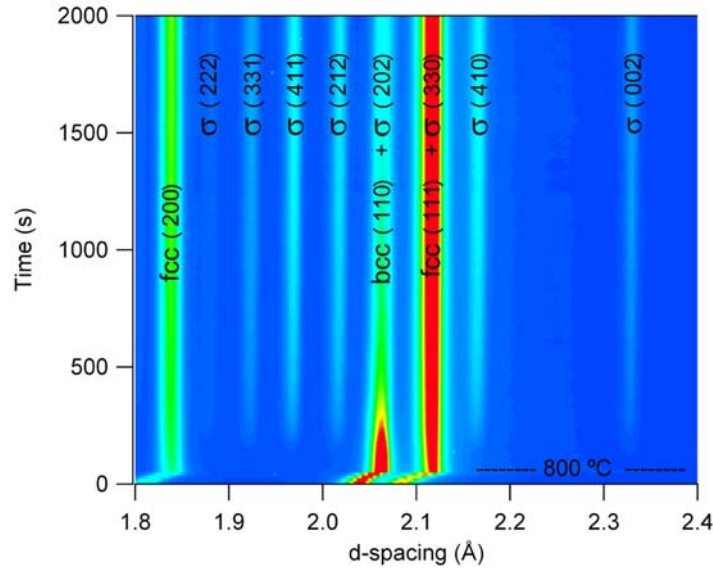
Figure 5: Pseudo-color plot (red corresponds to the highest intensity, blue corresponds to the lowest intensity) of high d-spacing diffraction peak intensities for the first 2000 s of the isothermal hold at 800ºC. The heating initiates at t=0 s, followed by a rapid increase in d-spacing of the peaks until the isothermal hold temperature is reached.
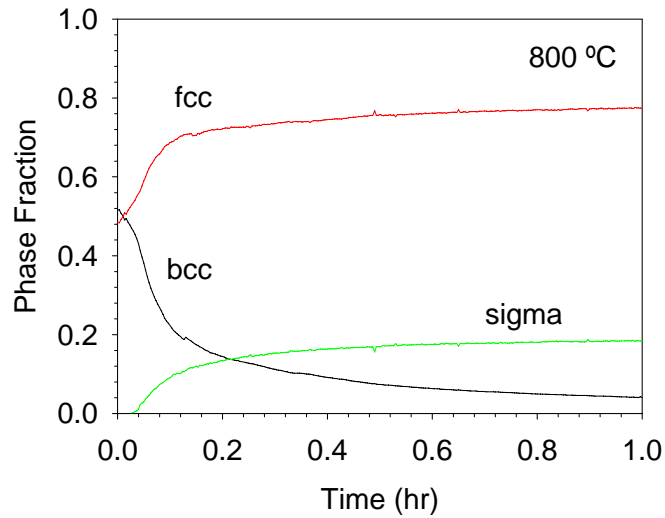
Figure 6: Summary of the measured fractions of the ferrite (bcc), austenite (fcc) and sigma phases as a function of time at 800ºC for times up to 1 hr.
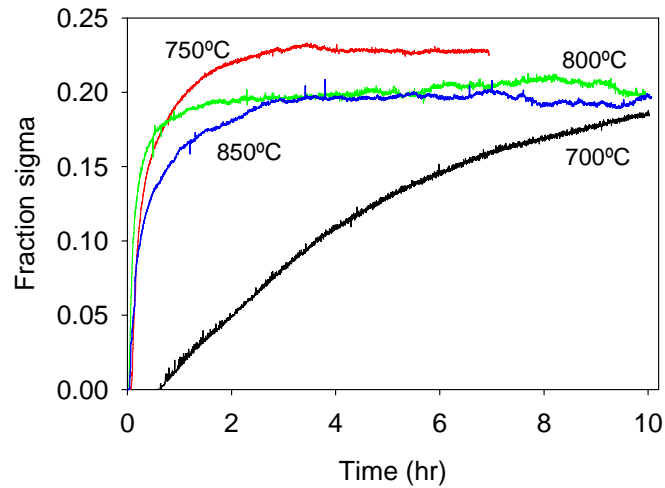
Figure 7: Results from the *in-situ* synchrotron measurements of sigma during the isothermal holds at each of the four temperatures.
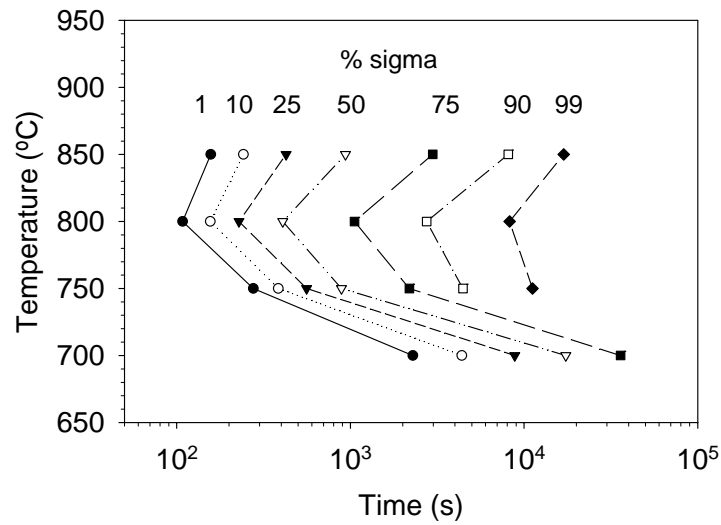
Figure 8: Plot showing the measured amount of sigma, relative to its equilibrium value, plotted versus log of the isothermal hold time at the 4 different temperatures. C-curve kinetics are apparent, with the nose occurring at approximately 800º C.
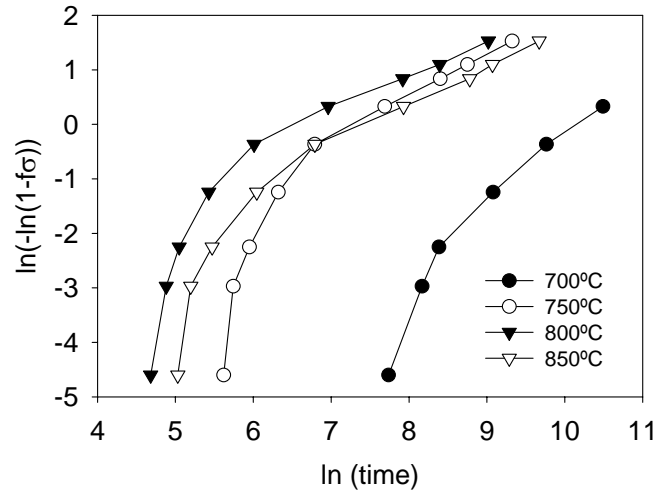
Figure 9: JMA plot of the sigma phase fraction plotted versus ln transformation time (s) at each of the four isothermal temperatures. The non-linearity suggests a change in the transformation mechanism between low and high fractions of sigma phase.
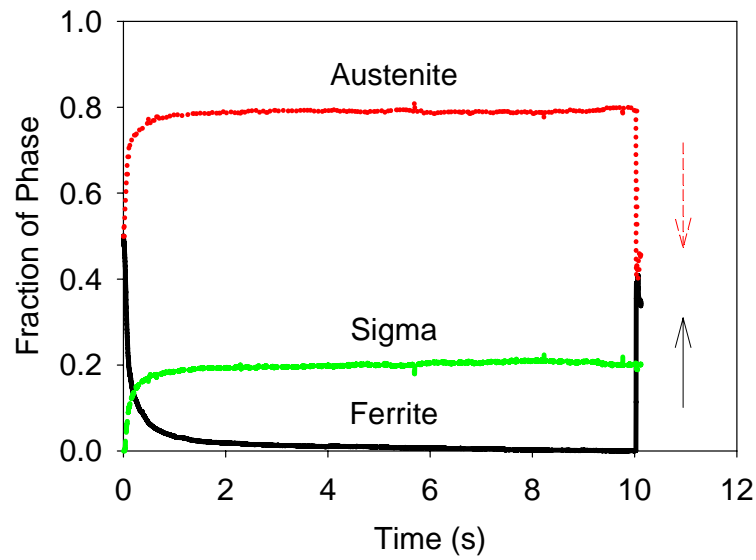

Figure 10: Measured ferrite, austenite and sigma phases for the entire run at 800ºC. The partial transformation of austenite to ferrite during the final cooling stage of the run is apparent, while the sigma phase was unaffected during cooling.
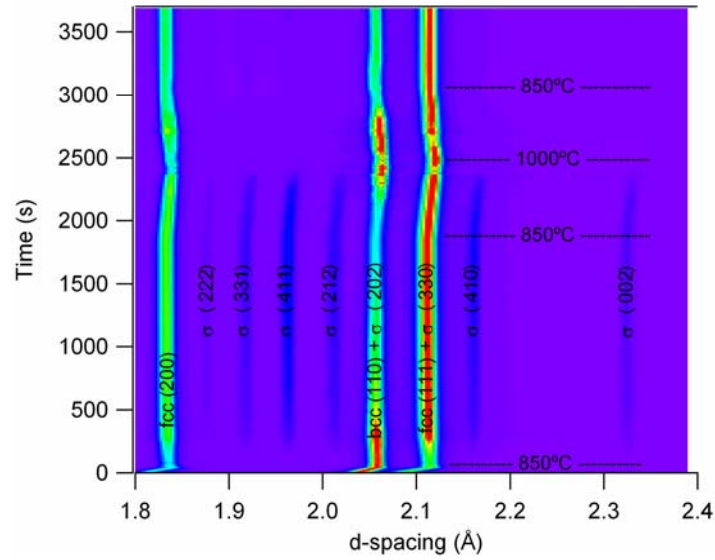
Figure 11: X-ray diffraction sequence for the first 3700 s of the run where the temperature was ramped to and from 1000°C.
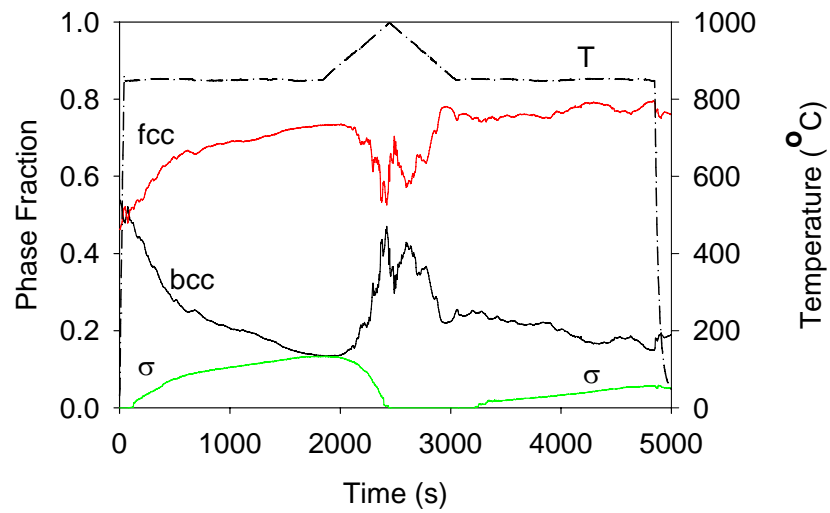

Figure 12: Measured fractions of ferrite (bcc), austenite (fcc) and sigma as a function of time. The temperature profile is indicated by the dashed line. Noise in the ferrite and austenite fractions appear at high temperatures when grain growth occurs and only a few grains satisfy the Bragg condition for diffraction.